Final Report

Project No. NR 358-269
Contract No. Nonr-471 (00)

A HIGH TEMPERATURE RADIATION CALORIMETER

By

Dr. Irving Johnson

Research Foundation
Oklahoma Agricultural and Mechanical College
Stillwater, Oklahoma

31 August 1953

Final Report

Project No. NR 358-269
Contract No. Nonr-471 (00)

A HIGH TEMPERATURE RADIATION CALORIMETER

By

Dr. Irving Johnson

Research Foundation
Oklahoma Agricultural and Mechanical College
Stillwater, Oklahoma

31 August 1953

Acknowledgments

The experimental work here reported was done on the whole by two men: Mr. William R. Willis and Mr. Wynn B. Fife. Mr. Willis carried the work during the first year and a half and Mr. Fife the last year. Mr. Willis had several part-time assistants during his period. These included Mr. Arnold Jensen and Mr. Philip Lewis.

We have had, during the entire research, the technical assistance of Mr. Gail I. Rutter, who, being a highly skilled mechanic, was able to transform into practical gagets, our various ideas. Mr. Rutter was an undergraduate mechanical engineering student. On the technical side we have also had the part-time help of Mr. Robert Anderson.

Miss Idress Cash, of the staff of the A. and M. College Art Department, made available the ceramic facilities of the College and also gave us advice on ceramic technics.

Mr. Charles Cole helped design and build the thyratron control circuit.

No report, however detailed, can adequately record the many hours of tedious work which have gone into obtaining data to support even a relatively minor conclusion. Weeks, even months, of careful work often lead up a blind alley. The experimental work of exploratory research, as here reported, never becomes routine. Mr. Willis and Mr. Fife have been both able and interested full partners in the experimental aspects of this research. Both Mr. Willis and Mr. Fife will use parts of this research as the basis for their Ph.D. theses.

HIGH TEMPERATURE RADIATION CALORIMETER

Introduction

It was the purpose of this research to investigate theoretically and experimentally the factors which are involved in direct calorimetry at high temperatures.

In particular, it was our purpose to study the operational characteristics of a spherically symmetrical calorimeter operating in a deep vacuum. The principle mode of heat transfer for such a calorimeter is radiation.

There are numerous uses for a calorimeter for making direct measurements at high temperatures. Studies of solid phase transformations and heat capacities of metastable phases are good examples where direct calorimetry is superior to the various indirect methods.

This report describes a spherically symmetrical calorimeter which was constructed. The experimental results are discussed in relation to the theory. Theory and experiment are shown to be in essential agreement.

This report is divided into three parts. In the first part, the experimental apparatus is described in detail. In the second part the theory of the calorimeter is presented. In the last part, the experimental results are described and compared with the theory.

EXPERIMENTAL APPARATUS

The experimental apparatus used for this research consisted of three basic parts plus the necessary electrical control and measuring components.

The three basic parts were (1) the spherical calorimeter proper (2) the spherical shield furnace and (3) the vacuum system. The electrical components were (1) potentiometer for measuring emfs developed by thermocouples (2) D.C. current source for internal heater (3) potentiometer for measuring current through internal heater (4) regulated A.C. source for shield heater (5) thyratron control circuit for regulating voltage to shield heater and (6) electrical controls of vacuum gauges.

The Calorimeter - The calorimeter was turned on a lathe from a piece of high purity graphite rod. A special fixture was constructed for the lathe which made possible the accurate turning of spherical forms of any size. The calorimeters used in this research were about two inches in diameter.

A hole was bored into the calorimeter and threaded. A graphite plug was turned and threaded to fit this hole. The internal heater fitted snugly inside this plug. Two small holes in the plug, lined with small pieces of clay pipe stem, allowed the electrical leads from the heater to be brought out of the calorimeter. Very high electrical insulation of the heater winding from the calorimeter was achieved using this method - the resistance between the heater winding and the graphite calorimeter being of the order of 200 megohms or greater.

The calorimeter thermel was fastened to the surface of the calorimeter using a graphite screw. The end of the thermel was just under the surface and hence did not "see" the shield wall. The thermel was not insulated from the calorimeter. Figure 1 shows a drawing of the calorimeter and the shield furnace.

The Internal Heater - The design of the internal heater shown in Figure 1 is but one of many different types which were tried in this research. The size and shape were varied. The size (gauge) of the Nichrome wire was varied. The heater was operated with a solid ceramic center with an empty center and with a center filled with a solid graphite plug. The space between the wire and the graphite plug was operated empty and packed with synthetic periclase.

The final design consisted of a thin lava cylinder upon which the #28 (B. & S.) Nichrome wire could be wound. The wire was held in place by means of a double thread. The wall thickness of the lava form was about 1/16". The center of the lava form was filled with a snug fitting graphite plug which made good contact with the calorimeter at one end and the threaded plug on the other end. The space between the wire and the plug was left empty since the periclase did not increase the heat transfer coefficient.

As will be seen, in the theoretical section which follows, the basic requirements for the heater are low effective heat capacity and good thermal contact with the calorimeter. Another constructional feature highly desirable is good thermal contact of the leads with the calorimeter. The need for this last requirement was not fully realized until all of the experimental work was finished.

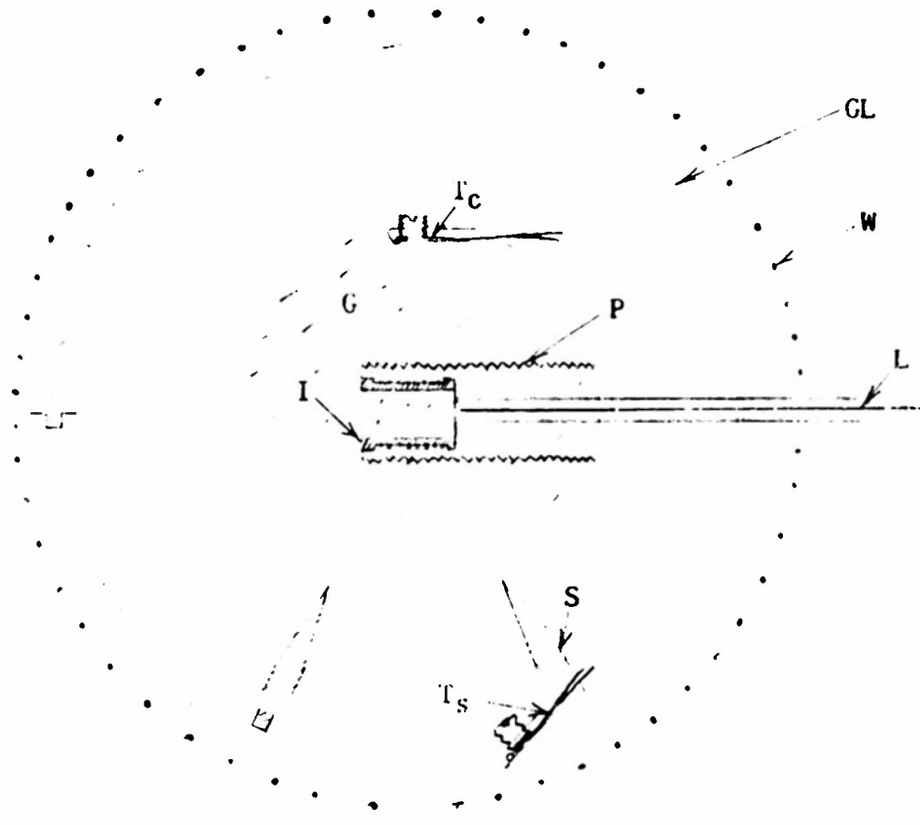

Figure 1 Calorimeter and Shield Furnace (Actual Size)

T_c Calorimeter Thermel

T_s Shield Thermel

G Graphite

P Plug

I Internal Heater

S Support

W Shield Heater Winding

GL Graphite Shield Liner

L Heater Leads

Shield Furnace - One of the most persistent problems throughout this research has been the method of constructing the shield furnace. The essential requirement was an isothermal spherical surface. The early shield furnaces used in this research were approximately spherical but very likely not isothermal. The final furnace, shown in cross section in Figure 1 fulfills both of these requirements very closely. Since the construction of a spherical furnace has apparently been a major reason for not using a spherically symmetrical design it would appear worth while to describe briefly the evolution of our furnace.

The first spherical shield furnace consisted of two ceramic hemishperes with a Nichrome heating wire fastened to the surface. These ceramic forms were made on a jigger using ordinary pottery clay. After the half shells had air dried, a loxodromic groove was machined on the outer surface. A special machine was designed and constructed to machine this groove. The Nichrome wire was held into the groove by means of fine wire ties. This furnace was used up to about 400°C which was its upper limit.

In an attempt to increase the upper temperature limit of the furnace, various insulating cements were tried. Of the many cements tried only ordinary furnace patching cement (Rutland) stuck to the ceramic forms during the curing cycle and subsequent heatings in the vacuum system. Even this cement eventually cracked off. With this insulation on the outside of the furnace the upper temperature limit was about 1200°C (the limit of the Nichrome wire).

We were not satisfied with these furnaces due to the fact that (1) it was difficult to fasten the shield thermocouple to the inner wall of the ceramic form, (2) it was impossible to be certain that the two half shells had not shifted relative to each other after the furnace was in the vacuum can, (3) it was almost certain that there was a cooler region around the equator where the two half shells came together and (4) it was difficult to make the ceramic forms of the same size and exactly spherical.

To solve these problems a graphite liner was made to fit inside of the ceramic furnace. This graphite liner could be turned exactly spherical on the lathe (our special fixture making this possible) and could be made with interlocking edges. Furthermore, the shield thermocouple could be screwed into a blind hole in this graphite liner thus assuring good thermal contact. The good thermal conductivity of the graphite would tend to equalize the temperature throughout the inner surface. Since entirely new ceramic forms were necessary for this furnace a new method for insulating the wire from the outside was tried. A thin ceramic semispherical shell of fire clay was made which could be slipped over the wire windings.

This furnace was used for several series of experiments but there was a disadvantage to this design. The lag between a change in heat input to the heater and the change in the shield temperature was too great - it was difficult to adjust the shield to a predetermined temperature. To decrease this lag, the final design was evolved.

The last shield furnaces used were made by laying on the outer surface of the graphite shells a thin (¼") layer of plastic alundum cement. After this layer had air-dried, it was carefully turned to a semispherical shape on the lathe. A loxodronic groove was then machined into the surface.

A preformed Nichrome winding was laid in this groove and tied on using thread. Another layer of alundum cement was then applied, allowed to air-dry, and turned to an exact semispherical shape. The whole piece was then heated in a muffle furnace to about 1100°C to cure the alundum cement.

From this description, it ought now to be obvious that the construction of a satisfactory spherical furnace is no longer a major hurdle to the use of spherical symmetry.

The use of the graphite liner gave rise to a new problem. While the vapor pressure of graphite is very low, it is finite and after several weeks of heating in a high vacuum, the entire contents of the shield furnace became coated with a very thin film of graphite. While the electrical resistance of this graphite film was large, nevertheless, there was an appreciable electrical conductivity from the calorimeter to the shield liner. This conductance path shorted the two thermocouples to each other. The resistance of this short, which was of the order of several megohms at room temperature, decreased to several thousand ohms at elevated temperatures. The emf developed by the thermels was irratic.

To keep the calorimeter electrically isolated from the graphite shield liner "film breakers" were placed on all connections from the calorimeter to the shield. The design of these "film breakers" and their method of operation may be seen in Figure 2. Only the carbon atoms approaching the film breaker within the rather small critical angle would enter the inside. Most of the atoms entering would deposit on the band just opposite the groove. The result was a break in the film, or at least a region where the film was very much thinner than at other places and had consequently a very high electrical resistance. For a period of about four weeks, during which the shield was continuously maintained at over 300°C, these film breakers were able to keep the calorimeter effectively insulated from the graphite shield liner.

Figure 2 Film Breaker
(Cross-section)

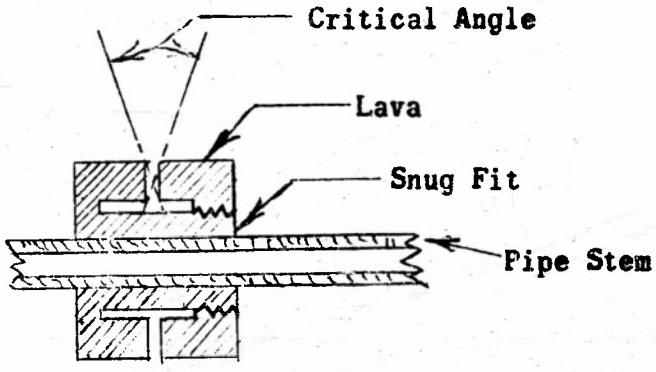

Vacuum System - The vacuum system in which the shield furnace was operated was constructed from steel pipe. Figure 3, drawn to scale, shows the main parts of the vacuum system. This all metal vacuum system evolved as our experience with high vacuum technic grew. The apparently large (4") pipe leading to the oil diffusion pump was necessary to give a rapid pumping speed in the working chamber. This was a dynamic system - the pumps operating continuously.

While this report is not the proper place for petty experimental details, it does seem appropriate to record some of the hard won high vacuum technics. Some of these technics are self evident - now. (1) A metal vacuum system is easily tested for leaks by applying pressure (10-15 p.s.i.) inside and using a soap - glycerine solution on likely spots for leaks. The addition

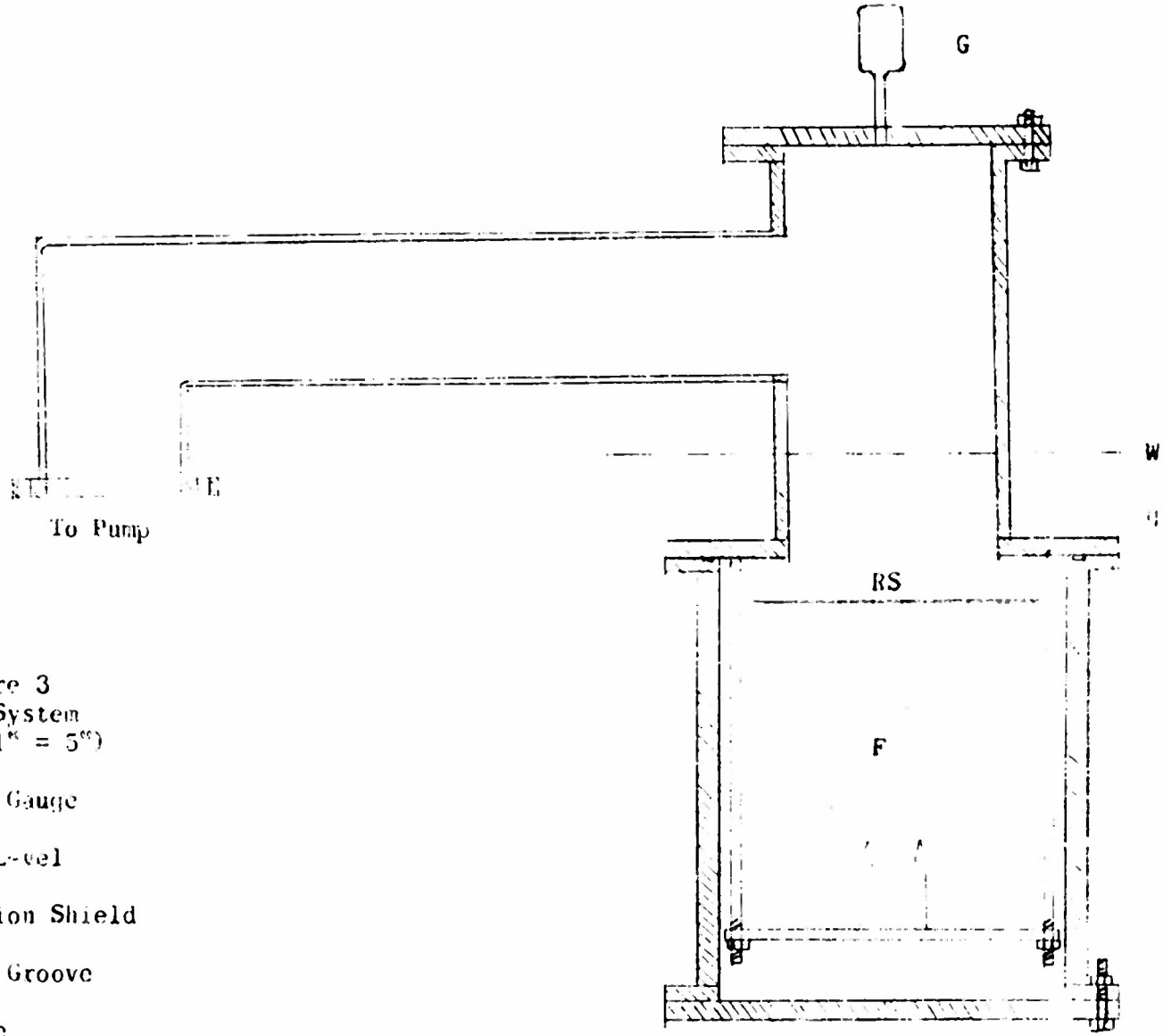

Figure 3
Vacuum System
(Scale: 1" = 5")

G Vacuum Gauge

W Water Level

RS Radiation Shield

g Gasket Groove

F Furnace

of glycerine enables one to apply a thin soap film on vertical surfaces. (2) The system should always be tested for leaks before pumping down. It takes much longer to find leaks by waiting until one can't seem to get a good vacuum. (3) Any connection or joint is a possible location for a leak. We found, after about a week of searching, a leak in the vacuum gauge! (4) Make permanent repairs on all leaks, soldering, welding, or brazing. (5) We did not find "glyptal" good for permanently repairing leaks. (6) Rubber gaskets, when placed in properly designed gasket grooves, are quite reliable ("O" rings are now available which would simplify assembly). (7) Connections may be made with ordinary pipe fittings only if the connections are also soft soldered. It is easy to take such joints down since the soft solder is easily melted with a hand torch. (8) One-eighth inch standard pipe fittings will hold a good vacuum if the threads are coated with glyptal before being assembled.

The pumps used for this apparatus consisted of an oil diffusion pump (D.P.I., Model MC 275) backed by a Cenco Megavac mechanical pump. After outgassing the system, pressures of 0.01 micron could be readily obtained at room temperature. It was possible to maintain pressures of less than 0.1 micron with the furnace operating up to 600°C.

So that the pumps could be operated continously a safety switch was installed in the A.C. line which powered the heater of the oil diffusion pump. This switch turned off the heater current if the water pressure dropped below a predetermined level. The unreliability of the services supplied to our laboratory made this and other safety features necessary.

Pressures were measured using a thermocouple type gauge (Hastings Model GV) at the fore pump and using a Philips gauge (D.P.I. Model PHG-1) on the top of the main vacuum chamber. The Philips gauge was not found to be reliable and is not recommended.

The electrical lead-ins for a metal vacuum system presented a problem. The solution was found after Stupakoff Kovar to glass seals were discovered. These glass to metal seals are available in almost any size or shape. It was found extremely difficult to make a rubber packing gland for leading wire out of a vacuum system and which was electrically insulated from the vacuum system.

The lead-ins for the thermocouples were designed to avoid contact of the platinum metal with other metals. The details of these lead-ins are shown in Figure 4. These lead-ins were not very reliable and had to be tested frequently for leaks since any motion of the thermocouple wire could crack the brittle picein cement.

The whole vacuum chamber was immersed in water in a galvanized tank. The temperature of the water was maintained approximately constant by allowing water to continuously flow through the tank.

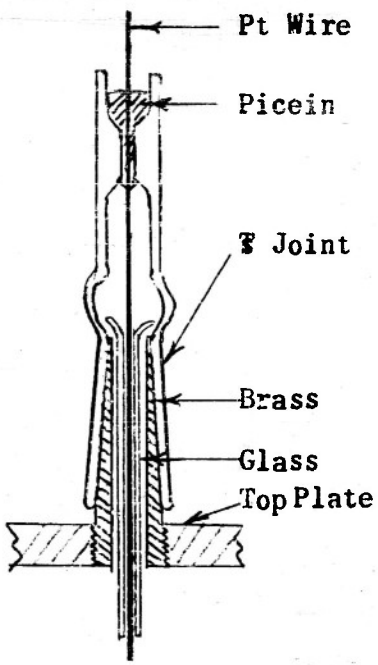

Figure 4 Thermel Leadins

Temperature Measurement: Early in the research Chromel - Alumel thermels were used. These thermels were not stable enough and so we changed to platinum, platinum - 13% rhodium thermels. The noble metal thermels have been quite satisfactory.

The thermel potentials were measured using a type K-2 (L. & N.) potentiometer. The galvanometer (L. & N. type 2284) had a sensitivity of about 0.045 micro volts per mm. An effective sensitivity of about 0.1 micro volts per mm was actually realized due to the fact that this research was done in rooms on the second floor of a temporary frame building.

The thermels were calibrated using the freezing points of standard samples of metals (obtained from the Bureau of Standards). The results of this calibration are given in Table 1. It is seen that the thermels differed by less than 2 micro volts from the standard tables. Two microvolts is about 0.2°C.

Table 1
Calibration of Thermels, Cold Junction 0°C.

Metal	Melting Point*	Observed emf's	
		Calorimeter	Shield
Tin	1.7504 mv. (231.9°C)	1.7490 mv.	1.7490 mv.
Lead	2.6624 mv. (327.3°C)	2.6607 mv.	2.6596 mv.
Zinc	3.6000 mv. (419.5°C)	3.5986 mv.	3.5987 mv.
Aluminum	6.2479 mv. (659.7°C)	6.2470 mv.	6.2488 mv.

* Values computed using N.B.S. standard tables for Pt, Pt-13% Rh thermels.

It was early noticed that the calorimeter thermel did not give the same emf as the shield thermel when the two were supposed to be at the same temperature. This difference was greater than the difference in calibration of the thermels. It was noted that the shield thermel had the larger emf in all cases when the graphite lined furnace was used. When the ceramic shield furnaces were used the potential difference between the shield and calorimeter thermels was either positive or negative. It was also noted that there was considerable AC pick-up by the shield thermel. This 60 cycle pick-up did not usually interfere with the potential measurements due to the fact that the period of the galvanometer was large.

The difference in potential between the shield and calorimeter thermels was positive when the graphite lined shield furnace was used. This difference ranged from 6 to 33 microvolts as the temperature of the shield varied from 600 to 900°k. This difference varied in an approximately linear manner with the temperature and had a temperature coefficient of about 0.1 $\mu v\ deg^{-1}$.

This temperature coefficient was too small for most thermal generated emfs. Possibly this potential arose from a rectifying action of the ceramic at elevated temperatures. Ceramic materials are known to become semiconductors at high temperatures.

Internal Heater Control - Like all other parts of the apparatus the internal heater control system underwent considerable modification as the system evolved. The final circuit was basically very simple as can be seen by Figure 5.

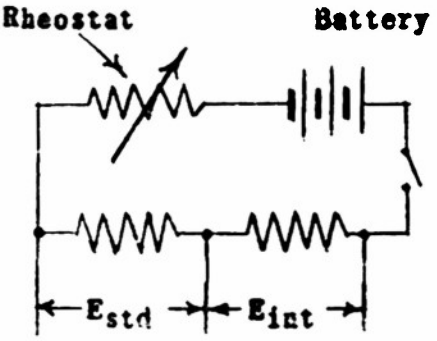

Figure 5 Internal Heater Circuit

Direct current from three automobile batteries operating in parallel was allowed to pass through a rheostat, a standard resistor and the internal heater all in series. The potential drop across the standard resistor and the internal heater could be measured using a potentiometer. The resistance of the standard resistor was 4.9711 ohms. The resistance of the internal heater varied with the design but was about five ohms. By keeping the batteries almost fully charged, it was possible to maintain the current through the heater constant ($\pm$0.1%) over long periods of time (1 to 2 hours).

The amount of heat being supplied by the heater was computed using the relation: $q = \frac{E_{std} \times E_{int}}{R_{std} \times 4.1833}$ Where q is the heat being generated by the internal heater in calories per second, E_{std} the potential drop (in volts) across the standard resistor, E_{int} the potential drop across the internal heater, R_{std} the resistance of the standard resistor and 4.1833 the factor to convert to calories (the potentiometer was calibrated in old practical units). The resistance of the two short pieces of copper wire which connected to the internal heater was approximately 0.02 ohms. This was considered negligible and no correction was made.

Shield Heater Control - The control of the shield heater is a problem which never was satisfactorily solved. The problem is one of constructing automatic control devices which will be sufficiently sensitive and able to cope with rather large thermal lags. Our best automatic device controlled the shield temperature to about $\pm$0.1°C which for a temperature of 500°C is 0.02%. This relatively high accuracy was not sufficient. It is believed that an accuracy of 0.001°C is needed.

The power for the shield was obtained from the AC lines. The variation of the voltage was much too great and so a voltage regulator was installed. The unit used had a capacity of 5KVA. (Superior Model EM 4106). The voltage was reduced to the amount required for the shield furnace by using a Variac (model V20). For some of the experiments a 1KVA voltage regulator was used (Superior Model IE 5101). This latter electronic regulator was more satisfactory.

Small adjustments of the heating current to the shield furnace were made using a thyratron control device. The circuit of the control device is shown in figure 6. The device operated by alternately shorting out resistor R_1. The length of time, during a cycle, that R_1 was shorted out could be controlled. The resistor R_1 was shorted out when the secondary of the transformer was shorted. This transformer was able to draw current during the part of the cycle the thyratron tube conducted. The portion of the cycle that the thyratron conducted depended on the phase between the control gird and the plate. This phase could be shifted by means of the phase shifting circuit (not shown in detail). The relative phase shift was controlled by applying a small (0 to 5 volts) DC voltage to the phase shift circuit. Thus, with this device, the amount of time the resistor R_1 was shorted could be varied from 50% to 0% of the time.

FG - 27

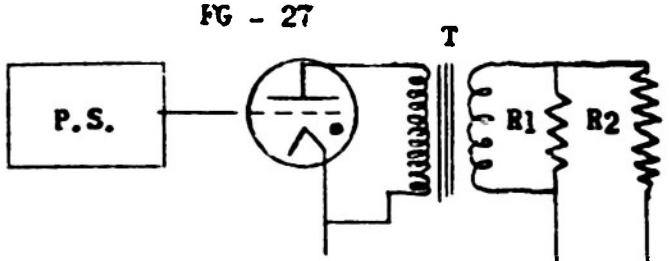

P.S. Phase Shifting Circuit

T Transformer

R_1 Resistor (2 ohms)

R_2 Furnace (12 ohms)

V Variac

Figure 6 Thyratron Control Circuit

The most successful automatic control device constructed derived the voltage for operating the phase shifting circuit by "observing" the position of a galvanometer light beam using two photoelectric cells as "eyes". These two photo cells were so arranged that when the galvanometer was at the null point the phase shift was maintained at some particular value. When the temperature went up, the galvanometer light beam moved (since the voltage of the thermel was balanced using a potentiometer) and thus more light was received by one of the photo cells. This changed the value of the voltage being supplied to the phase shifting circuit. The resistor, R_1, was then not shorted out as much of the time. This control device was able to control the temperature to within about $\pm 0.1°C$. The oscillations of the system were caused by excessive thermal inertia in the system.

By regulating the voltage to the phase shifting circuit manually it was possible to maintain the temperature constant to within $\pm 0.001°C$ during calibration experiments. During cooling experiments the regulation was usually not better than $\pm 0.01°C$. This degree of control (during cooling) was not believed sufficient.

THEORY OF CALORIMETER

Heat Transfer - The rate of transfer of heat q_{cs} from the surface of a sphere of radius R_c whose temperature is T_c to a concentric spherical surface of radius R_s and temperature T_s is given by the equation:

$$q_{cs} = \sigma A_g (T_c^4 - T_s^4) + k_n (T_c - T_s) \qquad (1)$$

Where $\sigma = 1.36 \times 10^{-9}$ cal/sec deg^4 cm^2 (Stefan - Boltzmann Constant), A = Surface area of inner sphere, k_n the thermal conductivity of the supports etc. of the inner sphere and g is given by the equation*:

$$g = \frac{e_c\, e_s}{e_s + e_c\,(1 - e_s)\,(R_c^2/R_s^2)} \qquad (2)$$

In equation (2) e_s and e_c are the emmissivities of the outer and inner surfaces respectively. Figure 7 shows the physical relations assumed.

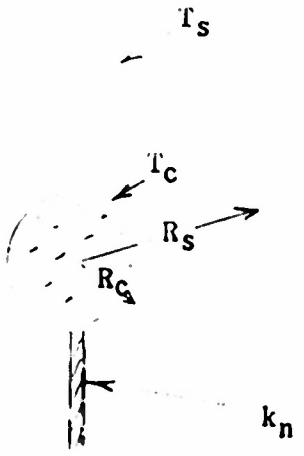

Figure 7 Basic Calorimeter (Schematic)

Equation (1) assumes that the space between the two spherical surfaces has been evacuated to a low enough pressure so that convectional heat transfer has been reduced to zero. Equation (1) thus assumes that the heat transfer is by radiation and ordinary newtonian conduction.

Equation (1) may be greatly simplified by noting that

$$T_c^4 - T_s^4 = 4T_a^3 \Delta T + T_a (\Delta T)^3 \qquad (3)$$

Where $\Delta T = T_c - T_s$ and $T_a = \frac{1}{2}(T_c + T_s)$. Since the second term on the right hand side of equation (3) is small compared to the first term, one may write in place of equation (1):

$$q_{cs} = (4 \sigma A_g T_a^3 + k_n) \Delta T = k_{cs} \Delta T \qquad (4)$$

Thus over a small range of temperatures (so that T_a does not vary too greatly) the rate of heat transfer is directly proportional to the temperature difference. This equation will be shown to be valid for the actual calorimeter which has been experimentally studied. It is seen that the rate of heat transfer will depend on the cube of the average temperature.

Cooling of a Perfect Conducting Sphere - If the inner sphere of Figure 7 is a perfect heat conductor, in which case the temperature will be constant throughout, the rate of cooling will be given by the equation:

$$-C \frac{dT_c}{dt} = q_{cs} \qquad (5)$$

Where C is the heat capacity of the sphere. If the approximate equation (4) is used for q_{cs} we obtain

$$-C \frac{dT_c}{dt} = k_{cs} (T_c - T_s). \qquad (6)$$

* A note on radiation heat transfer, by G. A. E. Godsave, Memo No. M.111 National Gas Turbine Establishment, March 1951.

If T_s maintained constant, then equation (6) may be integrated and the result is

$$\ln\ (T_c - T_s) = \ln(T_c^{\,o} - T_s) - \frac{k_{cs}}{C}\ t \qquad (7)$$

or

$$T_c - T_s = (T_c^{\,o} - T_s)\ \exp(-k_{cs}\ t/C) \qquad (7')$$

Where $T_c^{\,o} = T_c$ when $t = 0$. Thus a perfectly conducting sphere will cool exponentially when losing heat by radiation and conductance to a constant temperature heat sink. If a graph of $\ln(T_c - T_s)$ vs t were made, then a straight line would be obtained whose scope would be $-k_{cs}/C$. This ratio k_{cs}/C, which has the dimensions of reciprocal time units (sec^{-1}), will be known as the time constant for the sphere. If k_{cs} can be computed or measured then C, the heat capacity of the sphere, could be computed from the time constant.

Equation (6) and consequently, equation (7) were obtained assuming the approximate equation (4). It is possible to use the more exact expansion for q_{cs}, (1), and carry through an approximate integration. If q_{cs} from equation (1) is substituted into equation (5) then one obtains after rearranging and simplification the differential equation:

$$\frac{dx}{(x^4 - 1) + a(x - 1)} = \frac{-\sigma A_g T_s^{\,3}}{C}\ dt \qquad (8)$$

Where $x = T_c/T_s$; $a = kn/\sigma A_g T_s^{\,3}$. This equation can not be exactly integrated to a simple function due to the fact that the denominator of the left hand side may not be factored. If one is only interested in values of x close to unity then an approximate integration may be easily carried through. For this latter case, one obtains:

$$\frac{1}{a+4}\ \ln\frac{(x-1)}{(x+1)} \qquad \frac{4}{(a+4)\sqrt{2a+4}}\ \tan^{-1}\left(\frac{2x}{\sqrt{2a+4}}\right) = \frac{\sigma A_g T_s^{\,3}}{C}\ t + I \qquad (9)$$

I is the integration constant. When $a = 0$ this expression (9) reduces to the result obtained when equation (8) is exactly integrated with $a = 0$. If the left hand side of equation (9) is called $F(x,a)$ then one may unite

$$F(x,a) = F(x_o,a) - \frac{\sigma A_g T_s^{\,3}\ t}{C} \qquad (10)$$

where $x = x_o$ when $t = 0$. Thus a graph of $F(x,a)$ vs t will give a straight line whose slope is $-\sigma A_g T_s^{\,3}/C$. Since the values of $F(x,a)$ require a value of "a" for their computation one would need to employ a method of successive approximations to use this equation for the computation of C. In testing the use of this equation, it was found that the values of the slope ($-\sigma A_g T_s^{\,3}/C$) was not very sensitive to "a". This equation enables one to actually compute g/C rather than C directly. A method does exist for the estimation of g and consequently if equation (8) were applicable to the experimental situation values of C could be computed.

Comparison of equations (9) and (7) show that the latter equation is sufficiently accurate for the present purpose.

Cooling of a Sphere whose Conductivity is Finite - The exact equation for the cooling of a sphere whose heat conductivity is not infinitely great is not simply derived. The difficulty arises because of the thermal gradient which may exist within the sphere. As a good first approximation one may replace the finite conducting sphere by an infinitely conducting

sphere (of heat capacity C) surrounded by a spherical shell whose heat conductivity is some finite value, k_c, but whose heat capacity is zero.

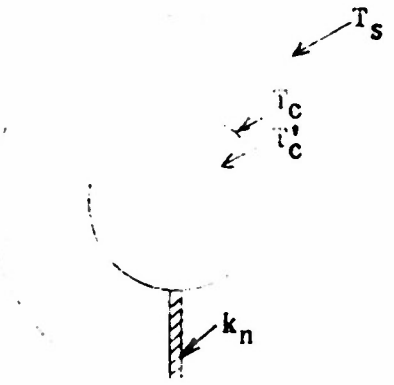

Figure 8
Calorimeter with finite Conductivity

Thus the rate of transfer of heat through the shell will be given by $q_{cs} = k_c(T'_c - T_c)$ (11) where T_c is the temperature on the outer surface of the shell. But q_{cs} is also given by equation (4) hence $k_c(T'_c - T_c) = k_{cs}(T_c - T_s)$ (12) from which one computes that

$$T'_c = T_c\left(1 + \frac{k_{cs}}{k_c}\right) - \frac{k_{cs}}{k_c} T_s \qquad (13)$$

If T_s is constant then

$$\frac{dT'_c}{dt} = \left(1 + \frac{k_{cs}}{k_c}\right) \frac{dT_c}{dt} \qquad (14)$$

and since equation (5) becomes

$$-C \frac{dT_c'}{dt} = q_{cs} \qquad (15)$$

for the case under consideration we obtain simply

$$-C\left(1 + \frac{k_{cs}}{k_c}\right) \frac{dT_c}{dt} = k_{cs}(T_c - T_s) \qquad (16)$$ which integrates to

give: $$\ln(T_c - T_s) = \ln(T_c^0 - T_s) - \frac{k_{cs}}{C} \frac{1}{\left(1 + \frac{k_{cs}}{k_c}\right)} t \qquad (17)$$

Thus a plot of $\ln(T_c - T_s)$ vs t will now have a slope of $-\frac{k_{cs}}{C} \frac{1}{\left(1 + \frac{k_{cs}}{k_c}\right)}$.

If -m is the slope of the plot the heat capacity is given by the equation:

$$C = \frac{k_{cs}}{m} \cdot \frac{k_c}{(k_c + k_{cs})} \qquad (18)$$

If k_c is large compared to k_{cs} the result will reduce to the same expression as obtained from equation (7). In general if $k_{cs}/m = C'$ then the true value of the heat capacity is obtained by multiplying the apparent heat capacity C' by a factor which is less than unity. Consequently the neglect of this factor will tend to give values of C which are too large. From equation (17) one predicts that a sphere with a finite conductivity will cool slower than one with infinite conductivity. This result is to be expected due to the fact that the outer surface temperature of a sphere with a finite conductivity will always be somewhat lower than the surface temperature of a sphere with an infinite conductivity. Since the surface temperature is lower, the rate of heat loss is also lower.

Cooling of a Sphere with an Internal Heater - Consider a spherical calorimeter with an internal heat source which is insulated from the calorimeter. If heat is being generated at the rate q_e, calories per second within the heat source, and if the rate at which heat is transferred from the internal heater to the calorimeter is q_{ic} then the heat balance equation on the internal heater is

$$q_e - q_{ic} - C_i \frac{dT_i}{dt} = 0 \qquad (19)$$

Where C_i is the heat capacity of the internal heater and T_i is the temperature of the internal heater. Under these same conditions the heat balance equation on the calorimeter may be written

$$q_{ic} - C\frac{dT_c}{d_t} - q_{cs} = 0 \qquad (20)$$

where C is the heat capacity of the calorimeter and the other symbols have already been defined. Assuming for q_{ic} and q_{cs} relations of the form of equation (4) we obtain

$$q_e - k_{ic}(T_i - T_c) - C_i\frac{dT_i}{dt} = 0 \qquad (21)$$

$$k_{ic}(T_i - T_c) - C\frac{dT_c}{dt} - k_{cs}(T_c - T_s) = 0 \qquad (22)$$

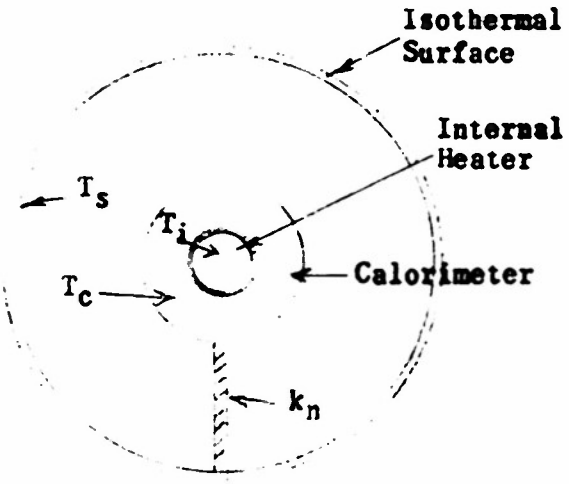

Figure 9

Calorimeter with Internal Heater

If T_s, the shield temperature, is constant, this pair of differential equations may be solved. Under steady state conditions one notes that $q_e = q_{cs}$. This allows one to evaluate, experimentally, q_{cs} as a function of T_c (if T_s is constant) and consequently to obtain the value of k_{cs}. Under cooling conditions q_e is zero. Under these conditions, the equation on the calorimeter temperature may be shown to be

$$(T_c - T_c^{\infty}) = \frac{(T_c^{0} - T_c^{\infty})}{(1 - \alpha)}\left(C^{m_1 t} - \alpha C^{m_2 t}\right) \qquad (23)$$

Where T_c^{∞} = calorimeter temperature when $t \to \infty$, T_c^{0} = calorimeter temperature when $t = 0$ m_1 and m_2 are the roots of the equation:

$$m^2 + \left(\frac{k_{ic}}{C_i} + \frac{k_{ic}}{C} + \frac{k_{cs}}{C}\right) m + \frac{k_{ic}\,k_{cs}}{C_i C} = 0 \qquad (24)$$

and $\alpha = m_1/m_2$. Both m_1 and m_2 are negative quantities, and since $-m_2$ is greater than $-m_1$ the quantity α is less than unity.

If a plot of $\ln(T_c - T_c^{\infty})$ is made, a curve similar to the full line of Figure 10 will be obtained. At sufficiently large times the curve will be a straight line of slope equal to m_1. This straight line will appear as though the calorimeter started at zero time at a higher temperature than actually observed. From the apparent value of this intercept, one may compute α.

Since m_1 is known from the slope, one may therefore compute both m_1 and m_2.

The quantity m_1 is given by the exact expression:

$$m_1 = \tfrac{1}{2}\left[-\left(\frac{k_{ic}}{C_i} + \frac{k_{ic}}{C} + \frac{k_{cs}}{C}\right) + \left\{\left(\frac{k_{ic}}{C_i} + \frac{k_{ic}}{C} + \frac{k_{cs}}{C}\right)^2 - \frac{4k_{ic}}{C_i} + \frac{k_{cs}}{C}\right\}^{\frac{1}{2}}\right] \qquad (25)$$

Since essentially three parameters are needed, i.e. k_{ic}/C_i; k_{ic}/C and k_{cs}/C and only two relations are known one may not directly compute these three parameters. Of the three numbers k_{ic}/C is the smallest. If this cross term k_{ic}/C is neglected (assumed zero) then one finds that $m_1 = -k_{cs}/C$ and $m_2 = -k_{ic}/C_i$. Since k_{cs} may be experimentally measured one may readily compute C, the heat capacity of the calorimeter. If k_{ic}/C is not assumed equal to zero then a simple calculation shows that:

$$-\frac{k_{cs}}{C} = m_1\left(1 + \frac{k_{ic}/C}{m_1 + k_{ic}/C_i}\right) \qquad (26)$$

Thus the values of C computed on the assumption that k_{ic}/C is zero will be too large.

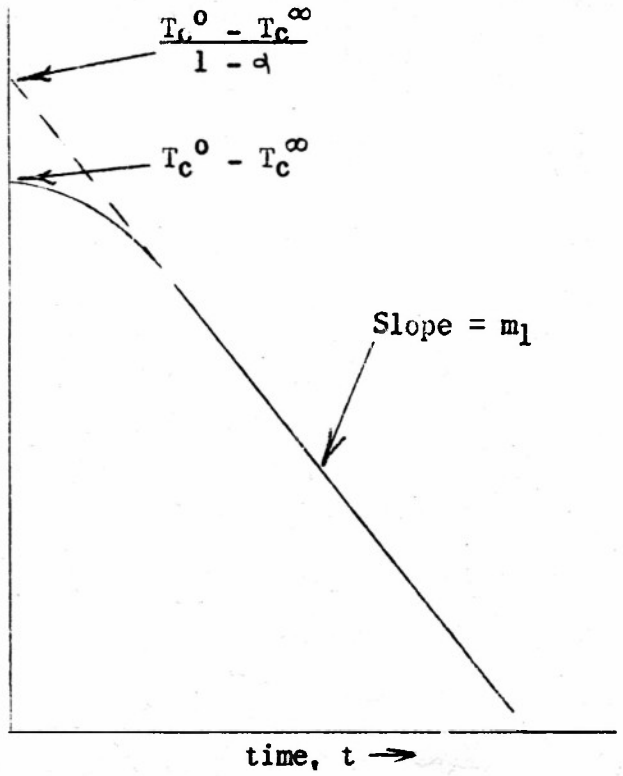

Figure 10
Cooling of Calorimeter with Internal Heater

Cooling of a Sphere with Varying Shield Temperature - The physical representation of the case under consideration is as shown in Figure 9. The differential equations for the internal heater and calorimeter will be equations (21) and (22) respectively. The heat balance on the shield will be given by the equation:

$$q_{cs} - C_s\frac{dT_s}{dt} + q_E - q_{se} = 0 \qquad (27)$$

where C_s is the heat capacity of the shield, q_E the rate heat is supplied by the internal wire winding of the shield heater and q_{se} the rate which heat is lost by the shield to its outer environment. This equation assumes that the thermal conductivity of the shield material is large. This assumption is probably not valid but will enable one to compute the largest possible effect of shield temperature variation on the cooling of the calorimeter. When q_{cs} is zero and a steady state exists, the value of q_E is equal to q_{se}. If then q_E is maintained at this value and if it is assumed that q_{se} does not change when T_s changes by small amounts then equation (27) may be written as follows:

$$k_{cs}(T_c - T_s) - C_s\frac{dT_s}{dt} = 0 \qquad (28)$$

where $k_{cs}(T_c - T_s)$ has been substituted for q_{cs}. If differential equations (21), (22), and (27) are solved simultaneously (with $q_e = 0$) the equation for the cooling of the calorimeter is found to be:

$$(T_c - T_c^\infty) = \frac{(T_c^o - T_c^\infty)}{(1 - \alpha)}\left[e^{m_1 t} - \alpha e^{m_2 t}\right] \qquad (29)$$

where $\alpha = m_1/m_2$ and

$$m_1 = \tfrac{1}{2}\left[-\left(\frac{k_{ic}}{C_i} + \frac{k_{ic}}{C} + \frac{k_{cs}}{C} + \frac{k_{cs}}{C_o}\right) + \sqrt{\left(\frac{k_{ic}}{C_i} + \frac{k_{ic}}{C} + \frac{k_{cs}}{C} + \frac{k_{cs}}{C_s}\right)^2 - 4\left(\frac{k_{ic}}{C_i}\frac{k_{cs}}{C} + \frac{k_{ic}}{C_i}\frac{k_{cs}}{C_s} + \frac{k_{ic}}{C}\frac{k_{cs}}{C_s}\right)}\right] \qquad (30)$$

m_2 is computed from an expression similiar to (30) but with negative sign before the radical.

If k_{ic}/C and k_{cs}/C are zero one finds that $m_1 = -k_{cs}/C$ and $m_2 = -k_{ic}/C_i$. These results are the same as obtained with the assumption that k_{ic}/C is zero and T_s is constant. Assuming k_{cs}/C_s is zero is equivalant to assuming an infinite heat capacity for the shield. This is the same as assuming that T_s does not change.

If as another limiting case of equation (28) one assumes only that k_{ic}/C is zero, then one finds that

$$m_1 = -k_{cs}\left(\frac{1}{C} + \frac{1}{C_s}\right). \qquad (31)$$

This result is of importance since it enables one to estimate the magnitude of the effect of a drifing shield temperature on the computed value of C. If m_1 is obtained from the limiting slope of a graph of log $(T_c - T_c^{\infty})$ is t then the value of C computed using equation (30) and assuming C_s is infinite would be actually smaller than the true value. Equation (31) shows that the rate of cooling can, under some circumstances, depend on both the heat capacity of the calorimeter and the shield furnace.

Cooling of a Sphere with a Leaky Internal Heater - The last cooling calculation of importance to the present study is the case of a calorimeter internal heater which leaks heat directly to the shield. The physical arrangement is shown in Figure 11. The direct heat leak from the internal heater to the shield might, in actual practice, be caused by the thermal conductance of the copper leads from the internal heater. This is probably a simplification of the actual situation but it will be sufficiently accurate for the present purposes. The basic heat balance equation on the internal heater and calorimeter will be the same as equations (19), and (20) but with an additional term $-q_{is}$ added to the left hand side of equation (19). The result of solving these two new differential equations is formally the same as equation (23) except that m_1 and m_2 have slightly different values. If it is again assumed that k_{ic}/C is small then one finds that

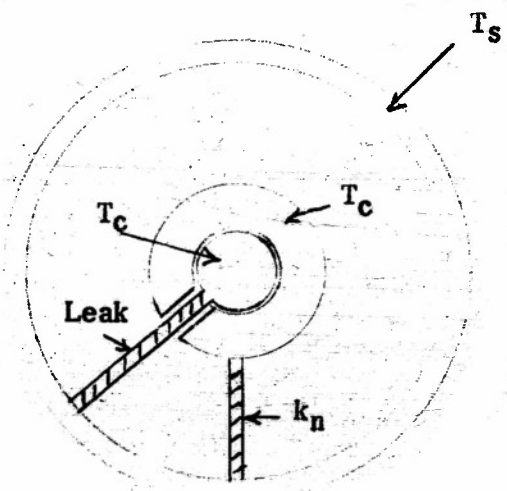

Figure 11
Calorimeter with Leaky Heater

$$m_1 = -\frac{k_{cs}}{C} \qquad (32')$$

and

$$m_2 = -\frac{(k_{ic} + k_{is})}{C_i} \qquad (32'')$$

In these equations k_{is} is the thermal conductivity of the leak from the calorimeter internal heater to the shield. It is of interest that this leak does not effect the value of the limiting value of the slope of log $(T_c - T_c^{\infty})$ vs t. As a matter of fact, since this leak actually makes m_2 more negative the influence of the stored heat in the internal heater on the cooling curve of the calorimeter is reduced.

EXPERIMENTAL RESULTS

The basic experimental data are of two kinds (1) calibration data and (2) cooling curve data. Calibration data consists of values of the calorimeter and shield temperatures for various different values of the heat input under steady state conditions. Sets of calibration data will differ from each other in the average temperature of the system. Cooling curve data consists of values of the temperature of the calorimeter and the shield as a function of time when the system is allowed to cool with zero heat input to the calorimeter. Cooling curves will differ as to the average temperature. In addition to these basic data various special measurements were made. These special measurements will be described as their need arises.

Calibration Data - Two kinds of calibration data have been obtained. In the first kind of calibration data, the heat input to the shield furnace (q_E) was maintained approximately constant, while in the second kind of calibration data the temperature (T_s) of the shield was maintained constant. Both q_E and T_s can not be kept constant for a set of calibration data. In general if q_E is kept constant T_s will increase when q_e (input to calorimeter heater) is increased. To maintain T_s constant for a set of calibration data q_E must be decreased very slightly for each successive larger value of q_e.

Steady State Heat Balance: - Since either type of calibration data are steady state measurements on the system the same basic equations will apply. These basic equations are obtained by setting all time derivatives in the general heat balance equations equal to zero. Under these conditions the equations are:

Internal Heater: $q_e - q_{ic} - q_{is} = 0$ (33)

Calorimeter: $q_{ic} - q_{cs} = 0$ (34)

Shield: $q_e + q_E - q_{se} = 0$ (35)

In these equations q_e & q_E are heat inputs (cal/sec) to the internal heater (calorimeter) and shield respectively q_{ic} and q_{is} are the rate of heat transfer from the internal heater to the calorimeter and the shield respectively. q_{is} is the "leak" from the internal heater to the shield. q_{cs} is the rate of heat transfer from the calorimeter to the shield while q_{se} is the rate of heat transfer from the shield to the environment. In general we will assume that any rate of heat transfer, q_{ij}, may be written in the form: $q_{ij} = k_{ij} (T_i - T_j)$ where k_{ij} is the heat transfer coefficient between i and j while T_i and T_j are the corresponding temperatures.

The behavior of the shield during calibration may be deduced from equation (35). If q_E is kept constant as q_e is increased then q_{sc} must increase if this equation is to remain valid. q_{se} can only increase if the shield's effective temperature for heat transfer to the environment increases. Thus T_s must increase as q_e is increased.

In the second kind of calibration data T_s is maintained constant and thus q_{se} is not allowed to increase. Equation (35) requires that q_E be decreased by an amount equal to the amount q_e has been increased. Since the values of q_e used were usually no greater than about 0.4 cal/sec. this would set the upper limit on the amount of adjustment which would need to

be made in q_E. The amount the temperature of the shield increases when q_e is increased with constant q_E depends upon the average temperature of the shield. At low temperatures the shield temperature increases about 23 degrees per calorie/sec. Thus for a value of q_e of 0.4 calorie/second the shield temperature would increase by about 9°C. The increase in shield temperature is found to be directly proportional to q_e. As the temperature increases the rate of increase in shield temperature with increase in q_e will be less.

Of fundamental importance is the experimental determination of q_{cs} as a function of T_c and T_s, combining equations (33) and (34):

$$q_{cs} = q_e - q_{is} \qquad (36)$$

If q_{is}, the heat leak to the shield were zero, then q_{cs} could be evaluated directly. However q_{is} is not zero. q_{is} is however, approximately proportional to q_e whence equation (36) may be written:

$$q_{cs} = q_e(1-a)$$

or

$$q_e = \frac{q_{cs}}{1-a} = \frac{k_{cs}}{1-a}\ (T_c - T_s) \qquad (37)$$

in equation (37) "a" is the proportionality constant in the equation $q_{is} = aq_e$. Equation (37) shows that a plot of q_e vs $T_c - T_s$ ought to yield a straight line whose slope is somewhat greater than k_{cs}. If "a" can be estimated then k_{cs} can be computed from the experimental calibration curve.

If q_{is} could be estimated directly, then the quantity $q_e - q_{is}$ could be plotted against $T_c - T_s$ and the heat transfer coefficient k_{cs} determined directly from the slope of the straight line. A method of estimating q_{is} would be to estimate the temperature of the internal heater wire and compute q_{is} by the equation $q_{is} = k_{is}\ (T_i - T_s)$. T_i may be estimated from the resistance of the internal heater wire using the equation:

$$R_t = R_o\ (1 + \beta(t - t_o)\ ) \qquad (38)$$

where R_t and R_o are the resistances at temperatures t and t_o respectively while β is the temperature coefficient of resistance (1.66×10^{-4} deg^{-1}) of the nichrome winding. The resistance of the wire of the internal heater may be computed from the measured voltage drop and current. Knowing $T_i - T_s$ one may compute q_{is} if the value of k_{is} is known. k_{is} may be estimated from the thermal conductance of the leads. The leads of the calorimeter were made of copper wire (B & S No. 28) and were approximately 4.13 cm long. Using 0.92 for the thermal conductivity of copper one computes k_{is} as approximately 3.6×10^{-4} cal sec^{-1} deg^{-1}. The data and calculations for a representative calibration curve are given in table 2.

Table 2

Estimation of Heat Leak from Internal Heater. Temperature 576°C.

q_e(cal/sec)	R (Ohms) heater	$T_i - T_s$°C	q_{is}(cal/sec)	q_{cs}(cal/sec)
0.0000	(5.8485)	0.00	0.0000	0.0000
0.0606	5.8510	2.53	0.0009	0.0597
0.2179	5.8570	8.67	0.0031	0.2148
0.3993	5.8624	14.28	0.0051	0.3942

If this estimate of q_{is} is correct then the error made in neglecting q_{is} is less than 2%. There is some uncertainity that the internal heater leads made sufficiently good thermal contact with the shield to be considered at the shield temperature at their extreme ends. If the ends of these leads operate at an appreciably lower temperature the heat leak will become significantly larger. These considerations would suggest that k_{cs}, as computed from the slope of the calibration curve might be too large by 2 to 10%. Redesign of the internal heater leads would allow this uncertainity to be greatly reduced.

Graphs were prepared of q_e vs $T_c - T_s$ for the calibration data obtained in this research. The data obtained in which the shield temperature was kept constant gave good straight lines. The constant q_E calibration data tended to show curvature. This curvature is likely caused by a slow drift in q_E.

From the graphs of q_e vs $T_c - T_s$ values of k_{cs} can be computed. According to equation (4), k_{cs} ought to be linear in the cube of the average temperature if k_n and g are not dependent on temperature. A graph of the values of k_{cs} vs T_a^3 showed that the data scattered rather badly around a straight line through the origin. As is seen in the figure (Fig. 12) there does not seem to be a regular trend in the data. It is believed that the scatter was caused by variation in k_n from one temperature to another caused by difference in the pressure in the system. No absolute check on the pressure was possible during all the experiments due to the fact that the Philips' gauge electronic control unit developed an electrical defect.

The slope of the straight line through the origin and the data is 3.47×10^{-10} (cal sec^{-1} deg^{-4}). According to equation (4) this quantity ought to be equal to $4\sigma A g$. Since $4\sigma A$ is known to be 4.41×10^{-10}(cal $sec^{-1} deg^{-4}$) one obtains 0.787 for g. When this value for g is substituted into equation (2) the emmissivity of the graphite surface is easily computed. Note that both surfaces are identical and hence the calculation may be made. One finds 0.824 for the emmissivity of the graphite surfaces. This value is reasonable for this substance. The fact that the value of the emmissivity is of the correct order of magnitude suggests that the basic theory is correct.

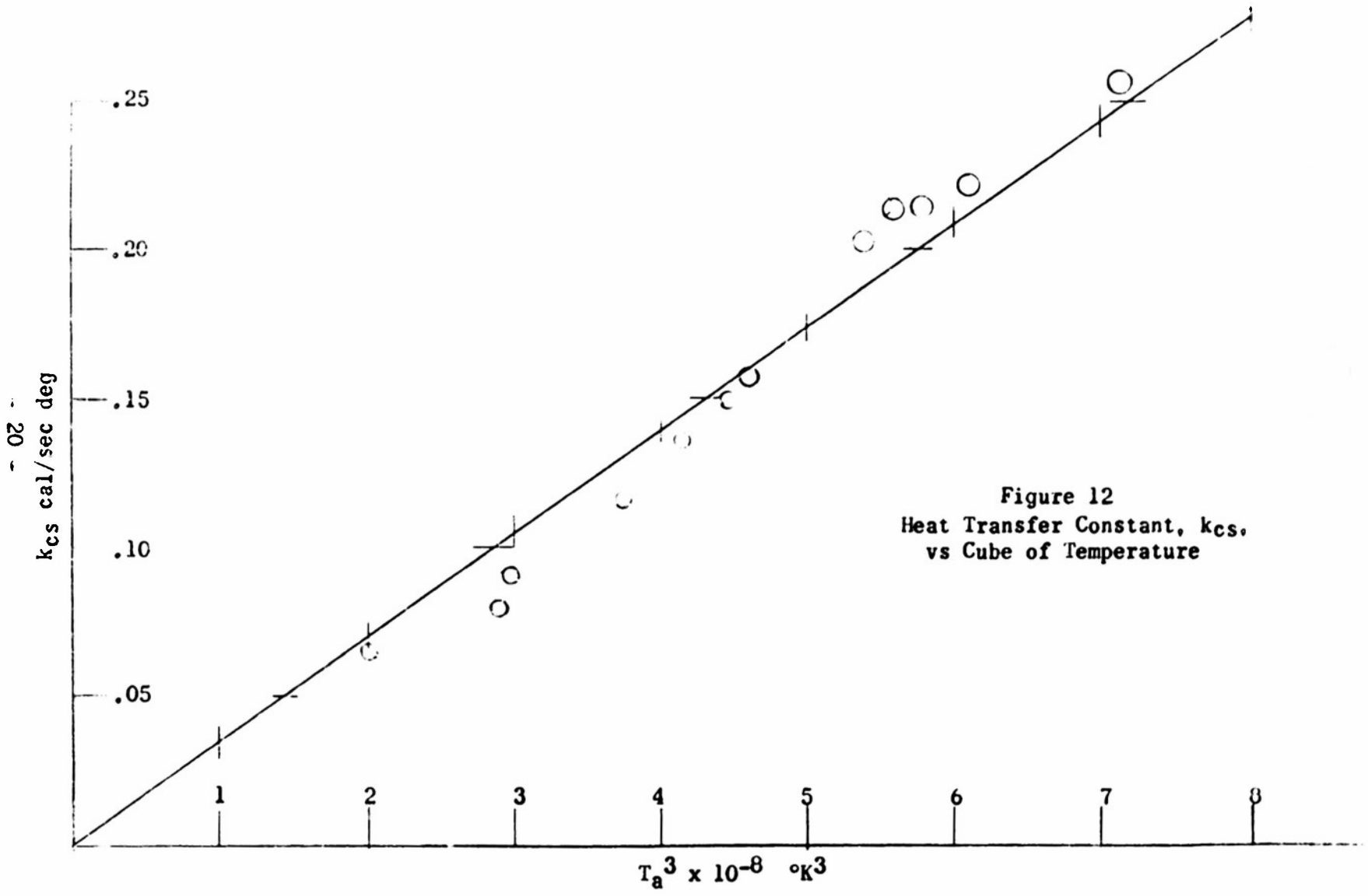

Figure 12
Heat Transfer Constant, k_{cs},
vs Cube of Temperature

Cooling Data - The cooling data obtained were of two kinds. The first kind was obtained at q_E constant while in the second kind the value of T_S was maintained constant. Both kinds of cooling curve data were similar during the initial part of the cooling interval. The two kinds of cooling curves differed during the latter part of the cooling interval. The constant T_S curves being characterized by a rapid asymptotic approach of the calorimeter temperature to the shield temperature. The constant q_E curves on the other hand appeared to be approaching the cooling curve for the shield.

According to the simple theory (equation (7)) a graph of log $(T_C - T_S)$ vs t ought to be a straight line. This is not found for the data of this research. Instead curves of the general shape of those shown in Figure 13 are obtained. Both curves are similar in shape at small times. Both curves leave the ordinate at zero time with zero slope. The slope gradually decreases. In the case of constant shield temperature, the slope becomes constant. In the case of the experiment at constant q_E the slope passes through a minimum (largest negative value) and then increases again.

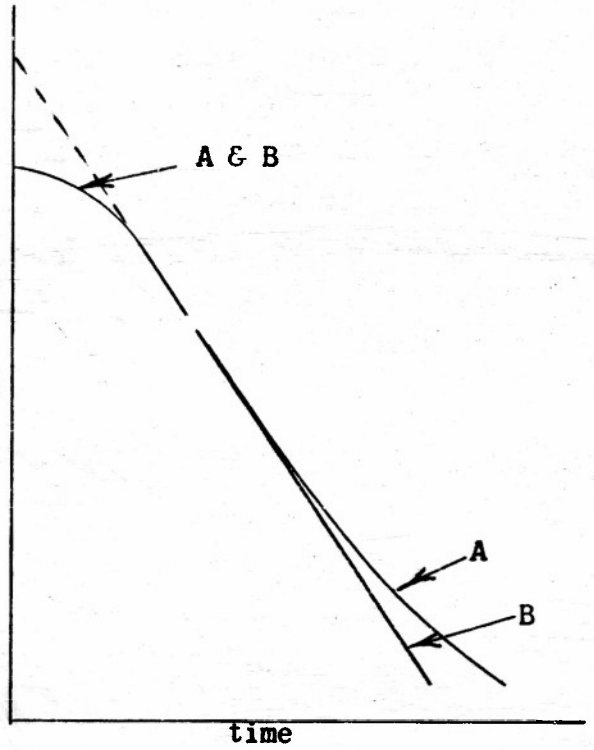

Curve A: q_E constant
Curve B: T_S constant

Figure 13

Experimental Cooling Curves

The failure of these curves to leave the ordinate at zero time with a finite slope is taken to be evidence for a thermal gradient existing between the internal heater and the calorimeter. At zero time, when the internal heater is turned off, the rate of heat transfer from the heater to the calorimeter does not immediately drop to zero. Rather, due to the fact that the heater has been operating above the temperature of the calorimeter, it will continue to furnish heat to the calorimeter at a rapidly decreasing rate. The time required for this heat source to become insignificant compared to the rate of heat transfer from the calorimeter to the shield will depend on the time constant of the internal heater. The time constant of the internal heater is numerically equal to the ratio of the heat capacity of the internal heater to the heat transfer coefficient between the internal heater and the calorimeter. The smaller this quantity the less influence the internal heater will have on the cooling curve of the calorimeter.

When the shield temperature is not kept constant during the cooling of the calorimeter it is found to decrease. This decrease is slow at first but after about a thousand seconds may become quite rapid. The reason the shield temperature drops is that the heat being supplied by the calorimeter has been decreased. Thus eventually the rate of decrease of the shield temperature can become equal to the rate of change of the calorimeter

temperature. When this occurs $T_c - T_s$ will remain constant for a short period and hence the graph of log (T_c-T_s) vs time will be parallel to the time axis. Even if the rate of decrease in T_s does not become equal to T_c the slope of the curve of log (T_c-T_s) vs t will gradually increase (become less negative). The curve, A, of Figure 13 shows this behavior.

The uncertainity of the magnitude of the influence of the drifting shield on the cooling curve of the calorimeter suggested that the constant q_E data were less useful for the computation of the heat capacity of the calorimeter than the constant T_s data. Consequently the detailed analysis has been confined to the data obtained at constant shield temperature.

The method of confronting the cooling curve data with theory was to plot the logarithm of the quantity $\Delta T_c = T_c - T_c^{\infty}$, where T_c is the temperature of the calorimeter at time t while T_c^{∞} is the temperature of the calorimeter when the cooling is complete, vs the time. The slope of the straight line portion of the curve gives according to the theory (equation (23)) the quantity-k_{cs}/C. The slope of the calibration curve, if proper connection for the heat loss from the internal heater is made, gives the quantity k_{cs}. Consequently one may compute the value of C.

In a typical experiment at about 663°K the slope of the straight line portion of the log ΔT_c vs t curve was found to be 2.16×10^{-3} (sec^{-1}). The corresponding calibration curve gave a value of 0.0901 (cal. sec^{-1} deg^{-1}). Therefore the heat capacity of the calorimeter is 41.7 (cal deg^{-1}) or since there were 9.435 moles of graphite an atomic heat capacity of graphite of 4.42 (cal deg^{-1} $mole^{-1}$). The values in the literature vary between 4.26 and 4.29. The experimental value ought to be slightly reduced for the small contribution of the internal heater (less than 1% of the total). More important is the possible error which exists in the value of k_{cs} since the calibration curve was not corrected for the leak from the internal heater. The experimental value differs by only 3.5% from the mean of the literature values. This amount is well within the uncertainity of the calibration curve.

Of less significance than the agreement of the heat capacity of graphite with the literature data is the agreement of the experimental data with the requirements of the quantitative theory developed above. The theory (equation (23)) predicts that the data ought to fit an equation of the basic form:

$$\Delta T_c = \frac{(\Delta T_c)_o}{1 - \alpha} \left(e^{m_1 t} - \alpha e^{\frac{m_1 t}{\alpha}}\right) \qquad (39)$$

where $(\Delta T_c)_o$ is the value of ΔT_c when t = 0. This equation has only two adjustable parameters α and m_1, both of which are easily obtained for any set of data by plotting the logarithm of ΔT_c vs t. The slope of the straight line portion gives m_1 directly (note that m_1 is a negative number) while the intercept of the straight line portion when extended to t = 0 gives the value of $(\Delta T_c)_o / (1 - \alpha)$ from which α may be easily computed. α is found to be a number smaller than unity. One may obtain a better value of m_1 from approximate values. This is done by dividing ΔT_c by $(\Delta T_c)_o / (1 - \alpha)$ and adding $\alpha e^{\frac{m_1 t}{\alpha}}$. The resulting quantity is called Y. The logarithm of Y is then plotted against t. The slope of the straight line through the data is m_1.

This procedure was applied to the data for the experiment reported above. The new value of m_1 found was 2.163×10^{-3} compared to 2.160×10^{-3}. In Figure 14 graphs are shown of both ΔT_c vs t and Y vs t on semilogarithmic paper. Note the excellent straight line found for the Y vs t plot.. It is of interest to note that the term $\alpha e^{\frac{m_1 t}{\alpha}}$ becomes smaller than 0.1%

Figure 14

Comparison of Experimental Data with Theory

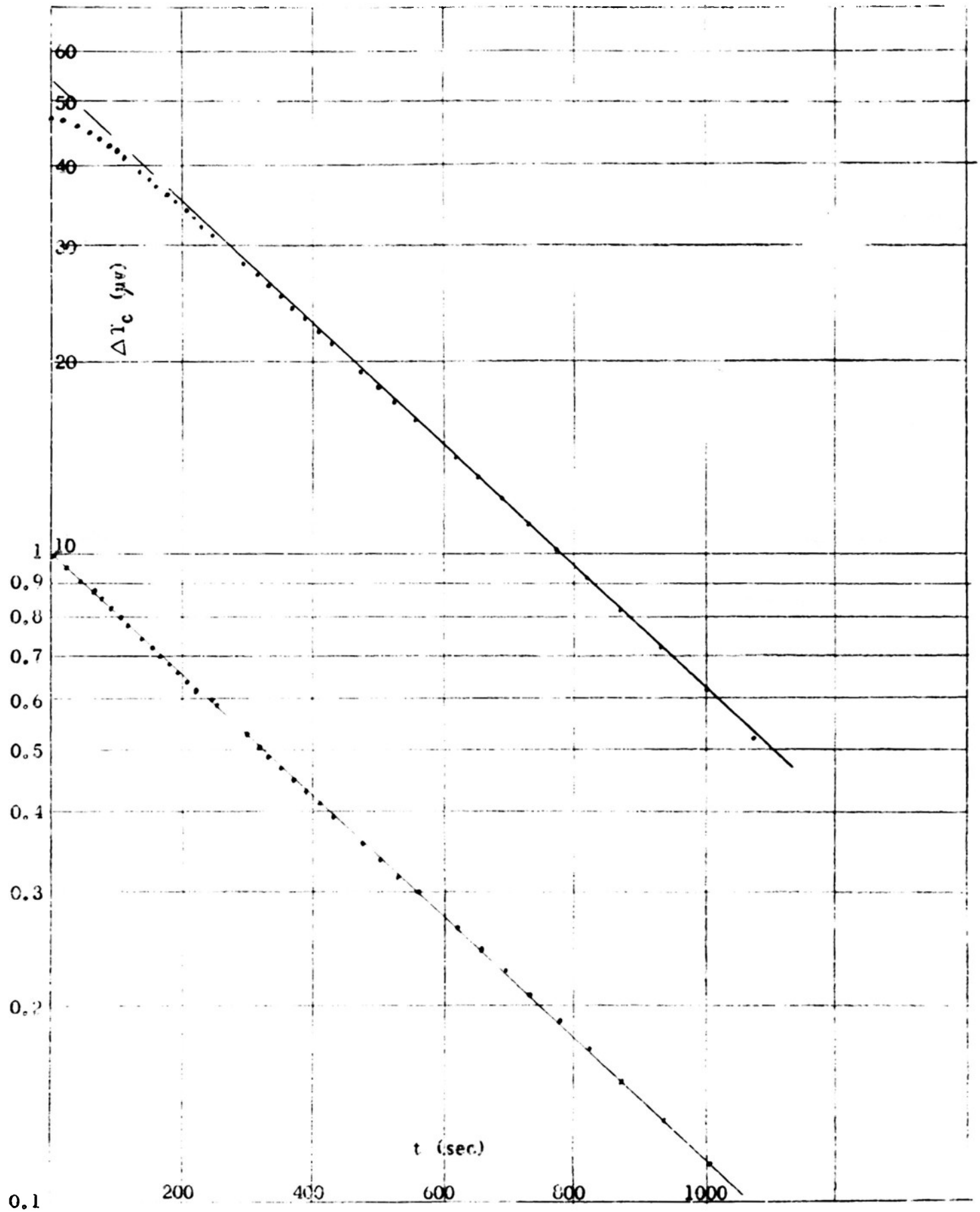

for a value of t of 315 seconds. The advantage of this last method of analyzing the data lay in the fact that all of the data may be used and especially the early values of ΔT_c which are actually the most accurately measured values. In addition the necessary condition that T_s is constant is more likely valid during the early part of the cooling curve.

Methods of Computing Heat Capacity - In addition to the method outlined above for the computation of the heat capacity of the calorimeter from the cooling curve data there are several other methods which have been used in this research.

A method much used in our early work was based on the equation (5):

$$-C \frac{dT_c}{dt} = q_{cs}$$

Where the quantities dT_c/dt and q_{cs} were obtained from the experimental data and then used to compute C. The values of dT_c/dt were measured on a large plot of T_c vs t. From the value of ΔT_c for each value of the measured slope the value of q_{cs} was determined from the calibration curve. As would be expected, from the description of the data, the values of C computed by this method started out, at short times, with very large values and then as the internal heater effect became less important decreased until the values were of the correct order of magnitude. Unfortunately when the values did level off then the effect of the shield variation became important. Also the accuracy of measuring the slope quickly decreased as the T_c vs t line leveled off. The basic error made in this method of computation is the neglect of the term q_{ic} which decreases slowly in magnitude as the calorimeter cools. Thus the value of q_{cs} used in this computation ought to be the quantity $q_{cs} - q_{ic}$ which will be smaller in all cases than q_{cs}.

This method was extensively used prior to the time that the experiments were made at constant shield temperature. When a cooling curve is taken with no control attempted on T_s one eventually reaches a practically constant rate of cooling and a constant difference between T_c and T_s. Therefore if q_{cs} is computed from this difference an approximately constant value of C will be obtained. This value of C will usually be smaller than the true value. The reason is seen in equation (31) which is applicable to the experimental situation here described.

Another method is based on a computation of the amount of heat lost by the calorimeter during a particular time interval and then dividing this heat quantity by the corresponding temperature change of the calorimeter. The net amount of heat lost by the calorimeter was obtained by graphical integration of a q_{cs} vs t graph. As might be expected this method gives high values of the heat capacity due to the fact that q_{ic} has again been neglected. In the calculation made, the integration was carried from zero time to 784 seconds, then from 84 seconds to 784 seconds etc. For each interval the mean heat capacity was computed. The results of this computation for a run at 813°K are given in Table 3.

Table 3

Integral Method of Computing Heat Capacity (313°K)

Interval	Total Heat	ΔT	C	$C_{corr.}$
0 - 784 sec	141.89 cal	2.53°C	56.1 cal/deg	50.4 cal/deg
84 - 784	110.21	2.35	46.9	43.8
136 - "	92.80	1.96	47.4	44.9
176 - "	80.91	1.76	45.0	44.0
236 - "	65.45	1.43	45.8	44.3
268 - "	58.01	1.29	45.0	43.7
312 - "	49.01	1.11	44.2	43.1
384 - "	36.27	0.837	43.3	42.6
400 - "	23.02	0.555	41.5	41.5

The mean literature value of the heat capacity for this temperature is 42.7 calories per degree. In the fifth column of Table 3 some values of the heat capacity of calorimeter computed from values of q_{cs} which have been approximately corrected for the heat lost by the internal heater. The value for the heat capacity of the internal heater was assumed to be 0.2 cal/deg. The rate of cooling of the internal heater was assumed to follow a simple exponential law. The correction was assumed to be insignificant after 400 seconds.

It is obvious that both the integral and differential methods require some estimate of the magnitude of the heat stored by the internal heater and also an estimate as to how rapidly this heat is lost. If one waits for the cooling to continue for three to four hundred seconds then the influence of the internal heater is insignificant. However, after this interval the temperature differences become too small to measure with accuracy.